

Mechanistic Insights into C–S Cross-Coupling Reactions Catalyzed by Nickel Bis(phosphinite) Pincer Complexes

Jie Zhang, Christopher M. Medley, Jeanette A. Krause, and Hairong Guan*

Department of Chemistry, University of Cincinnati, P.O. Box 21072, Cincinnati, Ohio 45221-0172, United States

Received August 20, 2010

Nickel bis(phosphinite) pincer complexes $[2,6-(R_2PO)_2C_6H_3]NiCl$ ($R = Ph$, **1a**; $R = Me$, **1b**; $R = ^iPr$, **1c**; $R = ^tBu$, **1d**) show catalytic activity in cross-coupling of aryl iodides and aryl thiols. The optimal catalytic conditions involve 1 mol % of **1a** and 2 equiv of KOH (with respect to aryl thiols) in DMF at 80 °C and tolerate a variety of functional groups in the substrates. The potential intermediates in these catalytic reactions, such as nickel thiolate complexes $[2,6-(Ph_2PO)_2C_6H_3]NiSAr$ ($Ar = Ph$, **2a**; $Ar = p-MeC_6H_4$, **3a**; $Ar = p-MeOC_6H_4$, **4a**), have been synthesized and spectroscopically characterized. The reaction between **2a** and PhI in DMF- d_7 is slow enough to argue against **2a** being directly involved in the C–S bond-forming step. NMR studies suggest that the pincer ligand framework in complexes **1a**, **3a**, and **4a** is destroyed by KOH via the cleavage of P–O bonds to release Ph_2POK , and further decomposition leads to Ph_3P and other phosphorus-containing products. The cross-coupling reactions are more effectively catalyzed by $Ni(COD)_2/Ph_2P(O)H$. The structures of **1b**, **2a**, **4a**, and $[2,6-(Ph_2PO)_2C_6H_3]NiP(O)Ph_2$ (**5a**), which is relevant to the decomposition process, have been studied by X-ray crystallography.

Introduction

Transition metal complexes bearing bis(phosphinite) POCOP-pincer ligands have become of increasing interest in homogeneous catalysis.¹ They are attractive for catalytic processes, in part due to their high thermal stability,² delicate balance of ligand electronics,³ and straightforward ligand synthesis.^{2a,4} As part of our ongoing efforts to develop catalytic reactions based on inexpensive metals such as nickel, we have studied the reactivity of a number of nickel complexes, including those derived from 1,3-bis(phosphinito)benzene

ligands (Figure 1).^{4d,5} We have recently shown that nickel hydrides, prepared from the reduction of **1c** and **1d**, catalyze the hydrosilylation of aldehydes and ketones^{5d} and the hydroboration of CO_2 .^{5c}

Catalytic cross-coupling of aryl halides and aryl thiols provides a simple and efficient route for the synthesis of diaryl sulfides (eq 1),⁶ which are of significant importance to the pharmaceutical industry.⁷ Palladium complexes have been reported to catalyze rapid C–S coupling reactions that are compatible with a wide variety of substrates.⁸ One of the

*To whom correspondence should be addressed. E-mail: hairong.guan@uc.edu.

(1) For a review on the catalytic applications of bis(phosphinite) pincer complexes, see: Morales-Morales, D. *Mini-Rev. Org. Chem.* **2008**, *5*, 141–152.

(2) (a) Göttker-Schnetmann, I.; White, P.; Brookhart, M. *J. Am. Chem. Soc.* **2004**, *126*, 1804–1811. (b) Göttker-Schnetmann, I.; White, P. S.; Brookhart, M. *Organometallics* **2004**, *23*, 1766–1776.

(3) Solin, N.; Kjellgren, J.; Szabó, K. *J. Am. Chem. Soc.* **2004**, *126*, 7026–7033.

(4) (a) Morales-Morales, D.; Grause, C.; Kasaoka, K.; Redón, R.; Cramer, R. E.; Jensen, C. M. *Inorg. Chim. Acta* **2000**, *300–302*, 958–963. (b) Bedford, R. B.; Draper, S. M.; Scully, P. N.; Welch, S. L. *New J. Chem.* **2000**, *24*, 745–747. (c) Hunks, W. J.; Jennings, M. C.; Puddephatt, R. *J. Inorg. Chem.* **2000**, *39*, 2699–2702. (d) Pandarus, V.; Zargarian, D. *Organometallics* **2007**, *26*, 4321–4334. (e) Naghipour, A.; Sabounchei, S. J.; Morales-Morales, D.; Canseco-González, D.; Jensen, C. M. *Polyhedron* **2007**, *26*, 1445–1448. (f) Olsson, D.; Arunachalampillai, A.; Wendt, O. F. *Dalton Trans.* **2007**, 5427–5433. (g) Solano-Prado, M. A.; Estudiante-Negrete, F.; Morales-Morales, D. *Polyhedron* **2010**, *29*, 592–600.

(5) (a) Gómez-Benitez, V.; Baldovino-Pantaleón, O.; Herrera-Álvarez, C.; Toscano, R. A.; Morales-Morales, D. *Tetrahedron Lett.* **2006**, *47*, 5059–5062. (b) Pandarus, V.; Zargarian, D. *Chem. Commun.* **2007**, 978–980. (c) Castonguay, A.; Spasyuk, D. M.; Madern, N.; Beauchamp, A. L.; Zargarian, D. *Organometallics* **2009**, *28*, 2134–2141. (d) Chakraborty, S.; Krause, J. A.; Guan, H. *Organometallics* **2009**, *28*, 582–586. (e) Chakraborty, S.; Zhang, J.; Krause, J. A.; Guan, H. *J. Am. Chem. Soc.* **2010**, *132*, 8872–8873.

(6) (a) Kondo, T.; Mitsudo, T. *Chem. Rev.* **2000**, *100*, 3205–3220. (b) Ley, S. V.; Thomas, A. W. *Angew. Chem., Int. Ed.* **2003**, *42*, 5400–5449. (c) Bichler, P.; Love, J. A. *Top. Organomet. Chem.* **2010**, *31*, 39–64.

(7) (a) Liu, G.; Huth, J. R.; Olejniczak, E. T.; Mendoza, R.; DeVries, P.; Leitz, S.; Reilly, E. B.; Okasinski, G. F.; Fesik, S. W.; von Geldern, T. W. *J. Med. Chem.* **2001**, *44*, 1202–1210. (b) Liu, L.; Stelmach, J. E.; Natarajan, S. R.; Chen, M.-H.; Singh, S. B.; Schwartz, C. D.; Fitzgerald, C. E.; O'Keefe, S. J.; Zaller, D. M.; Schmatz, D. M.; Doherty, J. B. *Bioorg. Med. Chem. Lett.* **2003**, *13*, 3979–3982. (c) Alcaraz, M.-L.; Atkinson, S.; Cornwall, P.; Foster, A. C.; Gill, D. M.; Humphries, L. A.; Keegan, P. S.; Kemp, R.; Merifield, E.; Nixon, R. A.; Noble, A. J.; O'Beirne, D.; Patel, Z. M.; Perkins, J.; Rowan, P.; Sadler, P.; Singleton, J. T.; Tornos, J.; Watts, A. J.; Woodland, I. A. *Org. Process Res. Dev.* **2005**, *9*, 555–569.

(8) (a) Kosugi, M.; Shimizu, T.; Migita, T. *Chem. Lett.* **1978**, *7*, 13–14. (b) Migita, T.; Shimizu, T.; Asami, Y.; Shiobara, J.; Kato, Y.; Kosugi, M. *Bull. Chem. Soc. Jpn.* **1980**, *53*, 1385–1389. (c) Schopfer, U.; Schlappbach, A. *Tetrahedron* **2001**, *57*, 3069–3073. (d) Li, G. Y. *Angew. Chem., Int. Ed.* **2001**, *40*, 1513–1516. (e) Li, G. Y.; Zheng, G.; Noonan, A. F. *J. Org. Chem.* **2001**, *66*, 8677–8681. (f) Murata, M.; Buchwald, S. L. *Tetrahedron* **2004**, *60*, 7397–7403. (g) Itoh, T.; Mase, T. *Org. Lett.* **2004**, *6*, 4587–4590. (h) Mispelaere-Canivet, C.; Spindler, J.-F.; Perrio, S.; Beslin, P. *Tetrahedron* **2005**, *61*, 5253–5259. (i) Fernández-Rodríguez, M. A.; Shen, Q.; Hartwig, J. F. *J. Am. Chem. Soc.* **2006**, *128*, 2180–2181. (j) Fernández-Rodríguez, M. A.; Shen, Q.; Hartwig, J. F. *Chem.—Eur. J.* **2006**, *12*, 7782–7796. (k) Fernández-Rodríguez, M. A.; Hartwig, J. F. *J. Org. Chem.* **2009**, *74*, 1663–1672. (l) Eichman, C. C.; Stambuli, J. P. *J. Org. Chem.* **2009**, *74*, 4005–4008. (m) Fu, C.-F.; Liu, Y.-H.; Peng, S.-M.; Liu, S.-T. *Tetrahedron* **2010**, *66*, 2119–2122.

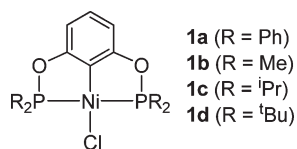
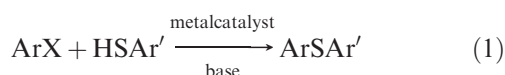


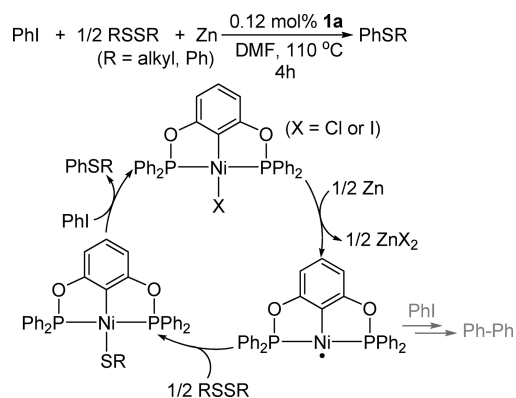
Figure 1. Nickel complexes with bis(phosphinite) POCOP-pincer ligands.

new challenges in the field is to replace palladium with inexpensive metals while still preserving high levels of efficiency and functional group tolerance. Although quite a few examples of Cu(I)-catalyzed C–S coupling reactions have been reported in the literature, high catalyst loadings and high reaction temperatures are often required.^{6b,9} Efforts have also been made to develop similar catalytic reactions using other inexpensive metals. Cheng and co-workers have recently demonstrated that aryl–sulfur bond formation is affected by 1 mol % of CoI₂(dppe) (dppe = 1,2-bis-(diphenylphosphino)ethane) in the presence of excess zinc metal.¹⁰ Iron will be even more attractive for its environmental friendliness; unfortunately, the reevaluation of a previously claimed iron system¹¹ for catalytic C–S coupling reactions has suggested that the actual catalyst might be the minute copper contaminant.^{12,13}



Nickel complexes may provide alternative solutions to catalytic C–S cross-coupling reactions because of their similarity with palladium complexes.^{6,14} To date, most reported nickel catalytic systems either suffer significant side

Scheme 1. Catalytic C–S Bond-Forming Reactions Reported by Morales-Morales et al. with a Proposed Reaction Mechanism



reactions¹⁵ and low isolated yields¹⁶ or require elevated temperatures.¹⁷ The most efficient nickel system is N-heterocyclic carbene (NHC)-based, where 1–4 mol % of catalyst has been used for the thiolation of aryl halides at 100 °C.¹⁸ To generate the proposed catalyst Ni(NHC)₂ and to minimize side reactions, a strong base such as KO^tBu may be employed. Cross-coupling of aryl iodides and thiols may also be catalyzed by simple nickel salts such as Ni(OAc)₂·4H₂O, Ni(NO₃)₂·6H₂O, and NiCl₂·6H₂O without any other supporting ligands.¹⁹ However, these reactions in general require a relatively high catalyst loading (5 mol %) and temperature (110 °C).

The Morales-Morales group has shown that nickel bis-(phosphinite) pincer complex **1a** catalyzes the thiolation of iodobenzene with various disulfides in the presence of zinc metal (Scheme 1).^{5a} They have proposed a mechanism involving a 15-electron Ni(I) radical and a nickel thiolate intermediate. In the case of PhSSPh (or a bulky dialkyl disulfide), the reaction between the Ni(I) species and PhI is thought to be competitive enough, resulting in the formation of biphenyl as the byproduct. We hypothesize here that the nickel thiolate intermediate could be accessible directly from the nickel halide complex and ArS[−] (generated from an aryl thiol and a base for the synthesis of a diaryl sulfide), thus bypassing the side reaction-prone nickel radical for an improved catalytic procedure. We are also intrigued by how the C–S bond is formed in Scheme 1: Does it involve oxidative addition of PhI to the nickel thiolate to generate a Ni(IV) intermediate, or does it go through a sigma-bond-metathesis type transition state? In this paper, we describe efficient cross-coupling of aryl iodides and aryl thiols catalyzed by air-stable nickel bis(phosphinite) pincer complexes **1a–d**. A typical catalytic reaction involves a low catalyst loading (1 mol %), operates at a mild temperature of 80 °C, and uses an inexpensive base such as KOH. We also report the synthesis, structures, and reactivity of nickel thiolate complexes that are potential intermediates in the catalytic cycles. Their stoichiometric reactions with PhI are, however, too slow to account for the rapid catalytic reactions. Instead, the nickel pincer complexes undergo decomposition under basic medium, and the coupling reactions are more likely to be catalyzed by the resulting secondary phosphine oxide-Ni(0) species.

(9) For recent examples, see: (a) Deng, W.; Zou, Y.; Wang, Y.-F.; Liu, L.; Guo, Q.-X. *Synlett* **2004**, 1254–1258. (b) Chen, Y.-J.; Chen, H.-H. *Org. Lett.* **2006**, *8*, 5609–5612. (c) Zhu, D.; Xu, L.; Wu, F.; Wan, B. *Tetrahedron Lett.* **2006**, *47*, 5781–5784. (d) Lv, X.; Bao, W. *J. Org. Chem.* **2007**, *72*, 3863–3867. (e) Carril, M.; SanMartin, R.; Dominguez, E.; Tellitu, I. *Chem.—Eur. J.* **2007**, *13*, 5100–5105. (f) Verma, A. K.; Singh, J.; Chaudhary, R. *Tetrahedron Lett.* **2007**, *48*, 7199–7202. (g) Sperotto, E.; van Klink, G. P. M.; de Vries, J. G.; van Koten, G. *J. Org. Chem.* **2008**, *73*, 5625–5628. (h) Herrero, M. T.; SanMartin, R.; Dominguez, E. *Tetrahedron* **2009**, *65*, 1500–1503.

(10) Wong, Y.-C.; Jayanth, T. T.; Cheng, C.-H. *Org. Lett.* **2006**, *8*, 5613–5616.

(11) Correa, A.; Carril, M.; Bolm, C. *Angew. Chem., Int. Ed.* **2008**, *47*, 2880–2883.

(12) Buchwald, S. L.; Bolm, C. *Angew. Chem., Int. Ed.* **2009**, *48*, 5586–5587.

(13) In a related study, cross-coupling of iodobenzene and an aromatic thiol was catalyzed by 0.1 mol % of CuO in the presence of 20 mol % of DMEDA (DMEDA = *N,N'*-dimethylethylenediamine) and 2 equiv of NaO^tBu. However, the reaction was performed at a high temperature (135 °C), and only a modest yield (76%) was reported. For details, see: Larsson, P.-F.; Correa, A.; Carril, M.; Norrby, P.-O.; Bolm, C. *Angew. Chem., Int. Ed.* **2009**, *48*, 5691–5693.

(14) The synthesis of aryl vinyl sulfides can be alternatively accomplished via catalytic hydrothiolation of alkynes. For nickel systems, see: (a) Ananikov, V. P.; Malyshev, D. A.; Beletskaya, I. P.; Aleksandrov, G. G.; Ereminenko, I. L. *Adv. Synth. Catal.* **2005**, *347*, 1993–2001. (b) Ananikov, V. P.; Orlov, N. V.; Beletskaya, I. P. *Organometallics* **2006**, *25*, 1970–1977. (c) Ananikov, V. P.; Zaleskiy, S. S.; Orlov, N. V.; Beletskaya, I. P. *Russ. Chem. Bull.* **2006**, *55*, 2109–2113. (d) Malyshev, D. A.; Scott, N. M.; Marion, N.; Stevens, E. D.; Ananikov, V. P.; Beletskaya, I. P.; Nolan, S. P. *Organometallics* **2006**, *25*, 4462–4470. (e) Beletskaya, I. P.; Ananikov, V. P. *Pure Appl. Chem.* **2007**, *79*, 1041–1056. (f) Beletskaya, I. P.; Ananikov, V. P. *Eur. J. Org. Chem.* **2007**, 3431–3444. (g) Ananikov, V. P.; Gayduk, K. A.; Orlov, N. V.; Beletskaya, I. P.; Khrustalev, V. N.; Antipin, M. Y. *Chem.—Eur. J.* **2010**, *16*, 2063–2071.

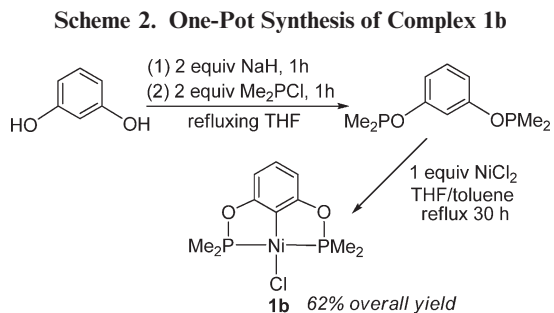
(15) (a) Takagi, K. *Chem. Lett.* **1987**, *16*, 2221–2224. (b) Percec, V.; Bae, J.-Y.; Hill, D. H. *J. Org. Chem.* **1995**, *60*, 6895–6903.

(16) Mollois, C.; Diaz, P. *Org. Lett.* **2000**, *2*, 1705–1708.

(17) Cristau, H. J.; Chabaud, B.; Chêne, A.; Christol, H. *Synthesis* **1981**, 892–894.

(18) Zhang, Y.; Ngeow, K. C.; Ying, J. Y. *Org. Lett.* **2007**, *9*, 3495–3498.

(19) Jammi, S.; Barua, P.; Rout, L.; Saha, P.; Punniyamurthy, T. *Tetrahedron Lett.* **2008**, *49*, 1484–1487.



Results and Discussion

Synthesis of Nickel Chloride Complexes. As the electronic and steric properties of bis(phosphinite) ligands may drastically impact the catalytic performance of the nickel POCOP-pincer complexes, we set out to synthesize nickel chloride complexes **1a–d** with different substituents on the phosphorus atoms. The new compound **1b** was isolated in good yield through a modified procedure from the one used for the preparation of **1a**,^{5a} **1c**,^{4d} and **1d**;^{5d} in this case bis(dimethylphosphinito)benzene was generated *in situ*, and its subsequent reaction with NiCl₂ was performed in the same reaction vessel for the ligand synthesis (Scheme 2). Both solid and solution samples of **1a–d** are stable indefinitely in air and, in addition, can be chromatographed on silica gel. Single crystals of **1b** were grown by adding *n*-hexane to a saturated CH₂Cl₂ solution of the complex. X-ray structure determination revealed two independent molecules in the lattice with minimal variation in conformation. One of the two structures is shown in Figure 2, and the crystallographic data are summarized in Table 1.

Catalytic Studies. After a series of experiments aimed at identifying the optimal conditions for Ni-catalyzed C–S coupling reactions, we discovered that the thiolation of iodobenzene was efficiently catalyzed by 1 mol % of **1a** in the presence of 2 equiv of KOH in DMF at 80 °C (Table 2, entry 2). Related nickel pincer complexes **1b–d** were less effective catalysts, and their relative catalytic activity seemed to follow the trend of steric congestion at the nickel center, i.e., a more sterically bulky R group on the phosphorus atoms led to a lower conversion (entries 3–5). A control experiment in the absence of any nickel species generated the sulfide product in merely 3% GC yield (entry 1), confirming that the cross-coupling reactions were primarily catalyzed by nickel. The choice of solvent was very critical, as the reaction in DMF was much more efficient than those in DMSO, THF, and toluene (entries 6–8). Replacing KOH with NaOH did not alter the reactivity significantly (entry 9), whereas the use of Cs₂CO₃, Na₂CO₃, K₃PO₄, or NaOMe slowed the catalytic reaction (entries 10–13). In principle, the reaction would require a stoichiometric amount of KOH; however, we found that using 1.1 equiv of KOH resulted in a much slower reaction than the one with 2 equiv of KOH. The reaction should be kept under an inert atmosphere despite the fact that all the reagents involved are air-stable; oxygen dissolved in the solution would oxidize PhSH to PhSSPh under the catalytic conditions,²⁰ causing a reduced GC yield.

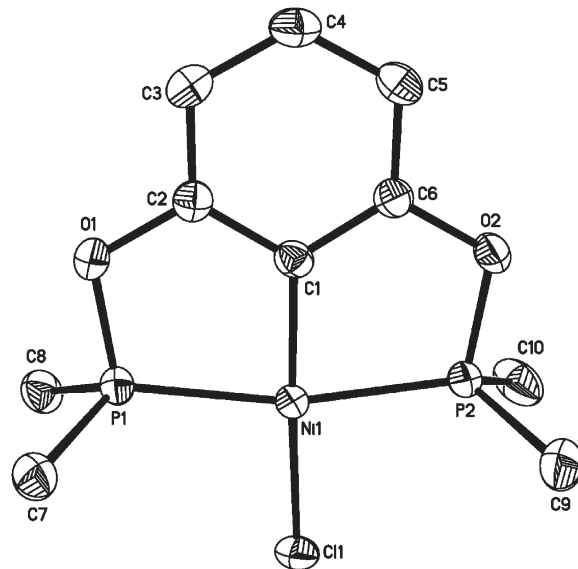


Figure 2. ORTEP drawing of [2,6-(Me₂PO)₂C₆H₃]NiCl (**1b**) at the 50% probability level. Hydrogen atoms are omitted for clarity. Selected bond lengths (Å) and angles (deg): Ni(1)–Cl(1) 2.1814(7), Ni(1)–C(1) 1.872(2), Ni(1)–P(1) 2.1477(7), Ni(1)–P(2) 2.1367(7), P(1)–Ni(1)–P(2) 165.24(3), P(1)–Ni(1)–Cl(1) 99.51(3), P(2)–Ni(1)–Cl(1) 95.22(3), C(1)–Ni(1)–Cl(1) 176.00(7).

With the optimized reaction conditions, we investigated the scope of this catalytic system. As shown in Table 3, the thiolation reactions were tolerant to functional groups such as MeO, CF₃, CN, and pyridine rings. All these cross-coupling reactions were highly efficient; the diaryl sulfides were isolated in high yields with no evidence of forming Ar–Ar (the homocoupling product from ArI) by GC. In a qualitative sense, the reactions were influenced by the *para*-substituents on the aryl iodides; they were accelerated by the electron-withdrawing groups (entries 5–7) and retarded by the electron-donating groups (entries 3 and 4). The cross-coupling of aryl iodides and 2-thionaphthol required a higher temperature (130 °C, entries 13–15), possibly due to the steric bulk of the naphthalene ring. Similar coupling reaction conditions for aryl bromides or aryl chlorides afforded only small amounts of coupling products.

Synthesis, Structures, and Reactivity of Nickel Thiolate Complexes. The proposed catalytic cycle in Scheme 1 would suggest that nickel thiolate complexes are involved in the C–S bond-forming step. We therefore independently synthesized these complexes from **1a** and the corresponding sodium thiophenoxides (eq 2), following a similar synthetic method developed for amido(diphosphine) (PNP-pincer) nickel complexes.²¹ Late transition metal complexes with nondative metal–heteroatom bonds are often unstable due to the repulsion between the heteroatom lone pair electrons and electrons in filled d-orbitals of the transition metals.²² On the other hand, the softness of thiolate ligands is well matched with late transition metals, contributing to the stabilization of M–S bonds. We found **2a–4a** were incredibly stable, as no decomposition was seen when the solid or

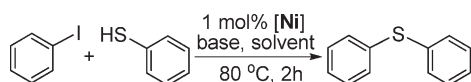
(20) (a) Carril, M.; SanMartin, R.; Domínguez, E.; Tellitu, I. *Green Chem.* **2007**, *9*, 315–317. (b) Saxena, A.; Kumar, A.; Mozumdar, S. *J. Mol. Catal. A: Chem.* **2007**, *269*, 35–40. (c) Dong, W.-L.; Huang, G.-Y.; Li, Z.-M.; Zhao, W.-G. *Phosphorus, Sulfur Silicon Relat. Elem.* **2009**, *184*, 2058–2065.

(21) Liang, L.-C.; Chien, P.-S.; Lee, P.-Y.; Lin, J.-M.; Huang, Y.-L. *Dalton Trans.* **2008**, 3320–3327.

(22) Caulton, K. G. *New J. Chem.* **1994**, *18*, 25–41.

Table 1. Summary of Crystallographic Data

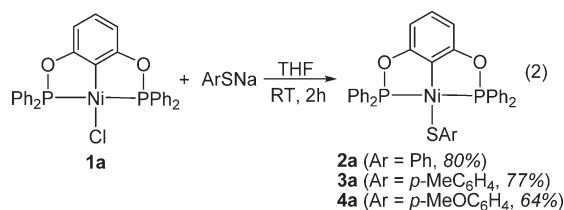
	1b	2a	4a (plates)	4a (needles)	5a · 1/2C ₆ D ₆
empirical formula	C ₁₀ H ₁₅ O ₂ P ₂ ClNi	C ₃₆ H ₂₈ O ₂ SP ₂ Ni	C ₃₇ H ₃₀ O ₃ SP ₂ Ni	C ₃₇ H ₃₀ O ₃ SP ₂ Ni	C ₄₅ H ₃₃ D ₃ O ₃ P ₃ Ni
fw	323.32	645.29	675.32	675.32	779.38
temp, K	150(2)	150(2)	150(2)	150(2)	150(2)
cryst syst	monoclinic	triclinic	monoclinic	monoclinic	triclinic
space group	<i>P</i> 2 ₁ / <i>c</i>	<i>P</i> $\bar{1}$	<i>P</i> 2 ₁ / <i>c</i>	<i>P</i> 2 ₁ / <i>c</i>	<i>P</i> $\bar{1}$
<i>a</i> , Å	9.1889(2)	11.6795(2)	14.8998(3)	9.1511(4)	12.3921(2)
<i>b</i> , Å	9.5488(2)	12.2924(2)	9.1421(2)	31.4575(12)	12.5039(2)
<i>c</i> , Å	31.4741(8)	12.5733(2)	24.1886(5)	13.4446(5)	13.0633(2)
α , deg	90	96.341(1)	90	90	82.995(1)
β , deg	90.509(1)	107.197(1)	107.532(1)	125.827(2)	77.215(1)
γ , deg	90	115.164(1)	90	90	67.787(1)
volume, Å ³	2761.52(11)	1501.43(4)	3141.81(11)	3138.0(2)	1825.83(5)
<i>Z</i>	8	2	4	4	2
d_{calc} , g/cm ³	1.555	1.427	1.428	1.429	1.418
λ , Å	1.54178	1.54178	1.54178	1.54178	1.54178
μ , mm ⁻¹	5.874	2.844	2.769	2.772	2.342
no. of data collected	23 095	12 886	25 959	25 460	15 774
no. of unique data	4968	5163	5631	5494	6304
R1, wR2 (<i>I</i> > 2 σ (<i>I</i>))	0.0311, 0.0796	0.0343, 0.0896	0.0364, 0.0926	0.0468, 0.1022	0.0336, 0.0861
R1, wR2 (all data)	0.0388, 0.0842	0.0400, 0.0939	0.0465, 0.0987	0.0903, 0.1205	0.0401, 0.0907

Table 2. Thiolation of Iodobenzene Catalyzed by Nickel Complexes **1a–d**^a

entry	[Ni]	base	solvent	GC yield (%)
1	no catalyst	KOH	DMF	3
2	1a	KOH	DMF	99
3	1b	KOH	DMF	78
4	1c	KOH	DMF	17
5	1d	KOH	DMF	6
6	1a	KOH	DMSO	7
7	1a	KOH	THF	8
8	1a	KOH	toluene	< 1
9	1a	NaOH	DMF	98
10	1a	CS ₂ CO ₃	DMF	14
11	1a	Na ₂ CO ₃	DMF	37
12	1a	K ₃ PO ₄	DMF	40
13	1a	NaOMe	DMF	81

^a Reaction conditions: 1.0 mmol of PhSH, 1.1 mmol of PhI, 2.0 mmol of base, and 1.0 mmol of *n*-decane (GC internal standard) in 6 mL of solvent.

solution samples of these complexes were exposed to air for days.



The nickel thiolate complexes tend to crystallize well, providing opportunities for X-ray diffraction studies. The single crystals of **2a** were obtained by layering a toluene solution of **2a** with pentane, whereas X-ray-quality crystals of **4a** came from the recrystallization of **4a** in CH₂Cl₂/hexanes, close inspection of which under a microscope revealed two different crystal forms: red-orange plates and orange needles. Structure determination of **2a** and **4a** showed slightly distorted square-planar coordination geometry for each nickel center (Figures 3–5). The P1, C1, P2, Ni, and S1

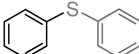
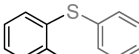
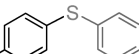
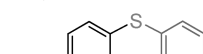
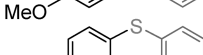
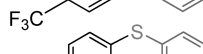
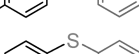
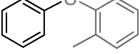
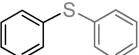
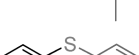
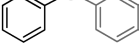
atoms almost lie in the same plane,²³ but, interestingly, the sulfur atom always swings toward one phosphorus arm. As a result, one P–Ni–S angle is significantly smaller than the other one ($\Delta\angle_{\text{P–Ni–S}}$ for **2a**, 6.97°; **4a**, plates, 9.00°; **4a**, needles, 12.11°). The Ni–P bond distances are also unequal with the one closer to sulfur being slightly shorter (Δd for **2a**, 0.0203 Å; **4a**, plates, 0.0151 Å; **4a**, needles, 0.0224 Å). These crystallographic features are possibly due to crystal-packing effects, and similar phenomena have been observed in other nickel thiolate complexes.²⁴ Although the plate and needle forms of **4a** have different orientations of Ph groups on P's (Figures 4 and 5) and different unit cell parameters (Table 1), key bond distances such as those for Ni–S(1) and Ni–C(1) are about the same. A striking structural difference between **2a** and **4a** is the dihedral angle (α) between P(1)–Ni–P(2) and Ni–S(1)–C(31) planes. The phenylthiolate group in **2a** is oriented in an almost perpendicular geometry relative to the coordination plane with an α of 72.76(5)°. In contrast, the 4-methoxyphenylthiolate ligand in **4a** is orientated in an “in-plane” geometry with a much smaller α (plates, 26.00(12)°; needles, 31.30(20)°). The origin of the difference in angles is unclear to us at the moment; it could be a result of crystal packing to maximize intra- and intermolecular π – π interactions between various aryl rings. In solution, the rotation of Ni–S bonds is not restricted, as all the thiolate complexes display a singlet in their ³¹P{¹H} NMR spectra. Another interesting variable parameter is the Ni–S(1) bond distance; the one in **2a** [2.2338(6) Å] is slightly longer than those in **4a** [plates, 2.1965(6) Å; needles, 2.1979(10) Å]. Nevertheless, these Ni–S bond distances fall in the typical range for square-planar nickel complexes with terminal aryl thiolate ligands.^{24,25}

With isolated nickel thiolate complexes, we were poised to investigate their reactivity toward PhI. A J. Young valve NMR tube containing **2a** (~0.03 M) and PhI (1.1 equiv) in DMF-*d*₇ was heated in a 80 °C oil bath for 24 h, after which

(23) The deviations from planarity of the least-squares plane defined by the P1, P2, Ni, and S1 atoms are calculated to be 0.0145, 0.0010, and 0.0104 Å for **2a**, **4a** plates, and **4a** needles, respectively. The C1 atoms are deviated from these planes by 0.0329, 0.0952, and 0.0698 Å for **2a**, **4a** plates, and **4a** needles, respectively.

(24) (a) Clegg, W.; Henderson, R. A. *Inorg. Chem.* **2002**, *41*, 1128–1135. (b) van der Vlugt, J. I.; Lutz, M.; Pidko, E. A.; Vogt, D.; Spek, A. L. *Dalton Trans.* **2009**, 1016–1023.

Table 3. Nickel-Catalyzed Thiolation of Aryl Iodides^a

		1 mol% 1a		2 equiv. KOH		DMF		Ar-SR	
entry	temp (°C)	time (h)	product	yield (%) ^b					
1	80	2		97					
2	80	2		94					
3	80	3		95					
4	80	3		96					
5	80	1		96					
6	80	1		97					
7	80	1		93					
8	80	2		94					
9	80	2		96					
10	80	2		97					
11	80	2		95					
12	80	2		95					
13	130	3		94					
14	130	9		91					
15	130	0.5		93					

^a Reaction conditions: 1.0 mmol of thiol, 1.1 mmol of aryl iodide, 0.01 mmol of **1a**, and 2.0 mmol of KOH in 6 mL of DMF. ^b Isolated yield.

³¹P{¹H} NMR spectroscopy showed almost no reaction and GC/MS analysis found a negligible amount of Ph₂S. The same but well-stirred solution (using protio DMF) in a Schlenk flask under otherwise the same conditions afforded Ph₂S with a 5% GC yield. A similar NMR reaction of **2a** with *p*-MeC₆H₄I in DMF-*d*₇ at 130 °C for 72 h produced *p*-MeC₆H₄SPh with a 25% NMR yield. The coupling product

(25) (a) Wenkert, E.; Shepard, M. E.; McPhail, A. T. *J. Chem. Soc., Chem. Commun.* **1986**, 1390–1391. (b) Krüger, H.-J.; Holm, R. H. *Inorg. Chem.* **1989**, *28*, 1148–1155. (c) Tucci, G. C.; Holm, R. H. *J. Am. Chem. Soc.* **1995**, *117*, 6489–6496. (d) Sánchez, G.; Ruiz, F.; Serrano, J. L.; Ramírez de Arellano, M. C.; López, G. *Eur. J. Inorg. Chem.* **2000**, 2185–2191. (e) Usón, M. A.; Llanos, J. M. *J. Organomet. Chem.* **2002**, *663*, 98–107. (f) Autissier, V.; Clegg, W.; Harrington, R. W.; Henderson, R. A. *Inorg. Chem.* **2004**, *43*, 3098–3105. (g) Cao, R.; Li, X.; Sun, H. *Z. Anorg. Allg. Chem.* **2007**, *633*, 2305–2309. (h) Gale, E. M.; Patra, A. K.; Harrop, T. C. *Inorg. Chem.* **2009**, *48*, 5620–5622.

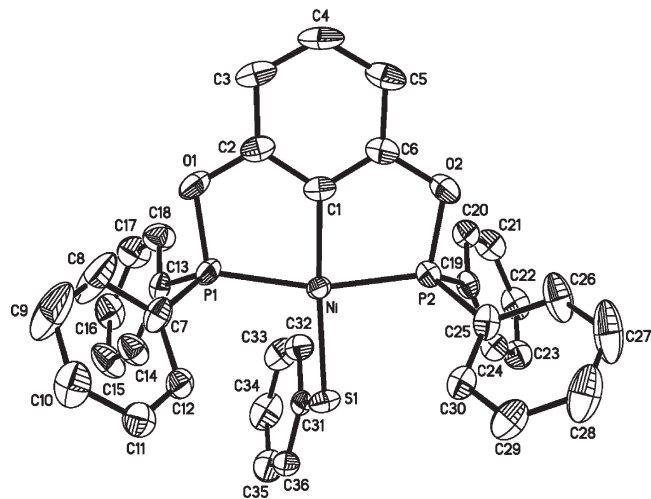


Figure 3. ORTEP drawing of [2,6-(Ph₂PO)₂C₆H₃]NiSPh (**2a**) at the 50% probability level. Hydrogen atoms are omitted for clarity. Selected bond lengths (Å) and angles (deg): Ni–S(1) 2.2338(6), Ni–C(1) 1.898(2), Ni–P(1) 2.1491(6), Ni–P(2) 2.1288(6), S(1)–C(31) 1.763(2), P(1)–Ni–P(2) 163.97(3), P(1)–Ni–S(1) 101.43(2), P(2)–Ni–S(1) 94.46(2), C(1)–Ni–S(1) 176.54(7), Ni–S(1)–C(31) 106.79(7).

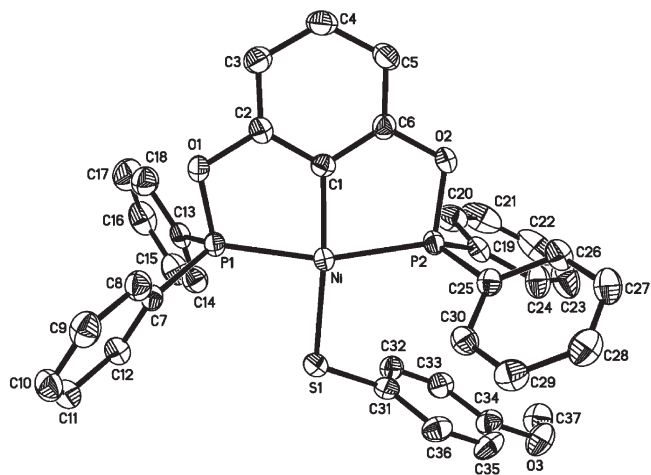


Figure 4. ORTEP drawing of [2,6-(Ph₂PO)₂C₆H₃]NiSC₆H₄OCH₃ (**4a**) (plates) at the 50% probability level. Hydrogen atoms are omitted for clarity. Selected bond lengths (Å) and angles (deg): Ni–S(1) 2.1965(6), Ni–C(1) 1.909(2), Ni–P(1) 2.1442(6), Ni–P(2) 2.1593(6), S(1)–C(31) 1.785(2), P(1)–Ni–P(2) 162.72(3), P(1)–Ni–S(1) 94.14(2), P(2)–Ni–S(1) 103.14(2), C(1)–Ni–S(1) 174.40(7), Ni–S(1)–C(31) 110.44(7).

was also confirmed by GC/MS. These studies suggested that C–S bonds could form directly from nickel thiolate complexes and aryl iodides; however, the stoichiometric rates are too slow to explain the facile catalytic reactions described above. We thus concluded that the reactions in both Scheme 1 and Table 3 should proceed via much more complicated mechanisms.

Reaction of Nickel Pincer Complexes with KOH. To gain further mechanistic information, we attempted to use ³¹P{¹H} NMR spectroscopy to detect the active nickel species under catalytic conditions. For the convenience of NMR studies, we used 10 mol % of catalyst **1a** for the coupling of PhI and PhSH with 2 equiv of KOH in DMF-*d*₇. The reaction mixture was heated at 80 °C and periodically

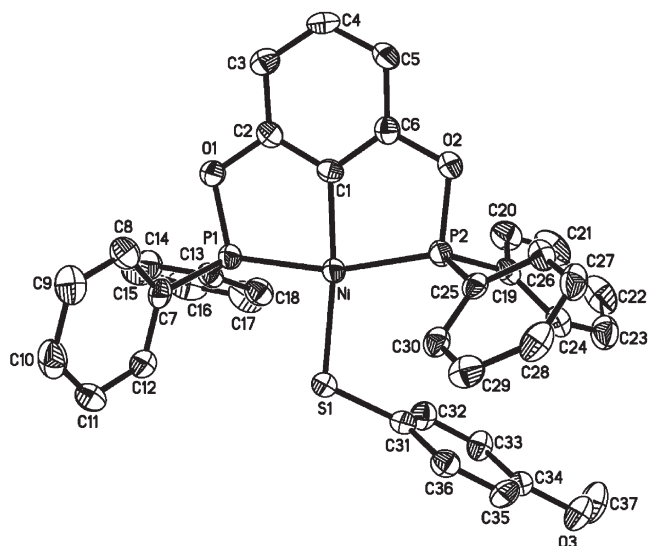


Figure 5. ORTEP drawing of $[2,6-(\text{Ph}_2\text{PO})_2\text{C}_6\text{H}_3]\text{NiSC}_6\text{H}_4\text{OCH}_3$ (**4a**) (needles) at the 50% probability level. Hydrogen atoms are omitted for clarity. Selected bond lengths (Å) and angles (deg): Ni–S(1) 2.1979(10), Ni–C(1) 1.907(3), Ni–P(1) 2.1389(11), Ni–P(2) 2.1613(11), S(1)–C(31) 1.782(4), P(1)–Ni–P(2) 163.96(5), P(1)–Ni–S(1) 91.93(4), P(2)–Ni–S(1) 104.04(4), C(1)–Ni–S(1) 172.99(11), Ni–S(1)–C(31) 111.28(12).

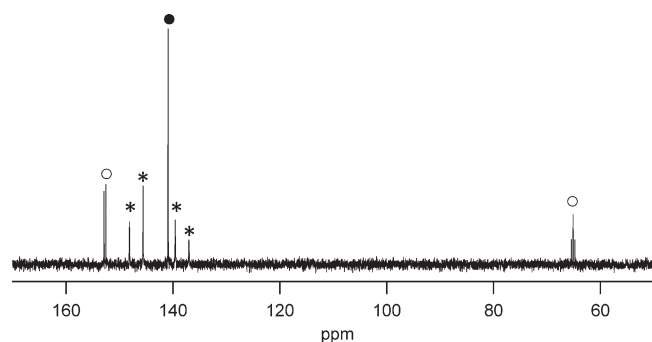


Figure 6. $^{31}\text{P}\{^1\text{H}\}$ NMR spectrum for the reaction of **1a** with KOH (4 equiv) in $\text{DMF-}d_7$ at 80°C for 2 h (● for **1a**, ○ for **5a**, * for **6a**).

cooled to room temperature for NMR analysis. In the initial stage of the reaction, the major nickel species was identified as **2a** (149.2 ppm), along with small amounts of other phosphorus-containing compounds. As more coupling products formed, the resonance of **2a** diminished while many other phosphorus resonances in the range from -10 to 50 ppm grew in. On the basis of these chemical shifts, we suspected that the pincer ligand framework might have been destroyed by KOH, forming new nickel complexes as the active catalysts. Our attention was then directed to the study of the interaction between KOH and various nickel complexes that are relevant to our catalytic system.

First, we treated **1a** with 4 equiv of KOH in $\text{DMF-}d_7$, and the resulting mixture was heated at 80°C for 2 h.²⁶ The $^{31}\text{P}\{^1\text{H}\}$ NMR spectrum (Figure 6) showed three nickel species (with a ratio of 43:17:40): the unreacted **1a** (140.9 ppm), a new complex **5a** featuring a doublet (152.7 ppm) and a triplet (65.1 ppm) with a coupling constant of 54 Hz, and another compound, **6a**, with an AB spin system (146.7 and

(26) KOH did not dissolve completely under this condition.

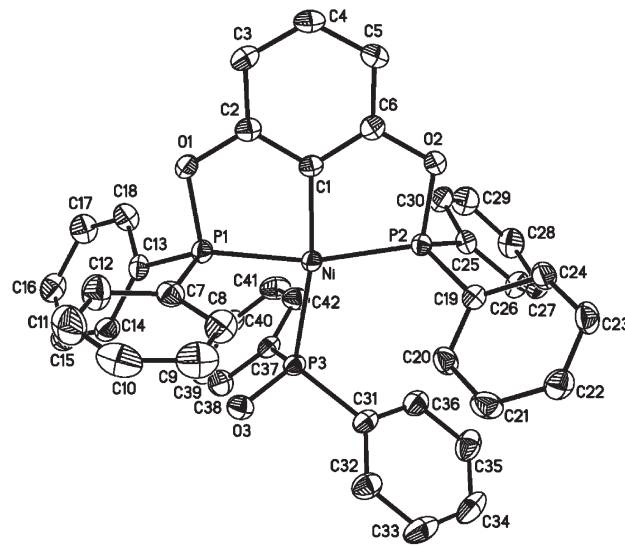


Figure 7. ORTEP drawing of $[2,6-(\text{Ph}_2\text{PO})_2\text{C}_6\text{H}_3]\text{NiP}(\text{O})\text{Ph}_2$ (**5a**) at the 50% probability level. Hydrogen atoms are omitted for clarity. Selected bond lengths (Å) and angles (deg): Ni–C(1) 1.9193(19), Ni–P(1) 2.1555(6), Ni–P(2) 2.1589(6), Ni–P(3) 2.2306(6), P(3)–O(3) 1.5145(15), P(1)–Ni–P(2) 161.20(2), P(1)–Ni–P(3) 89.59(2), P(2)–Ni–P(3) 107.68(2), C(1)–Ni–P(3) 170.75(6).

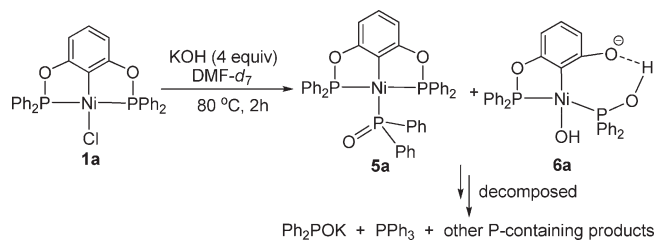
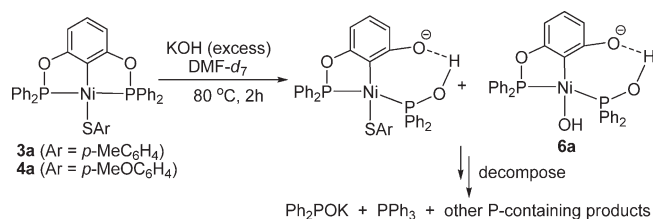
138.5 ppm, $J_{\text{AB}} = 413$ Hz). Complex **5a** is consistent with a nickel complex bearing a P-bonded $\text{Ph}_2\text{P}(\text{O})^-$ ligand as well as two equivalent P nuclei and thus assigned as $[2,6-(\text{Ph}_2\text{PO})_2\text{C}_6\text{H}_3]\text{NiP}(\text{O})\text{Ph}_2$. This compound was independently synthesized from **1a** and Ph_2POK and characterized by NMR, IR, and X-ray crystallography (Figure 7), but its rapid decomposition upon standing precluded further characterization with elemental analysis and mass spectroscopy. Nevertheless, its presence in the reaction mixture implied the release of Ph_2PO^- from the pincer ligand. The AB pattern in Figure 6 suggests that **6a** contains two inequivalent P nuclei, but still in the form of a phosphinite-type ligand due to the chemical shifts in the low-field region. We have yet to successfully synthesize this compound independently; however, we propose that one of the P–O bonds in **1a** is cleaved by KOH, resulting in a seven-membered ring with a hydrogen-bonding interaction (Scheme 3). Related chemistry was observed in ruthenium complexes bearing pyridine-based bis(phosphinite) PONOP-pincer ligands, except that in that case H_2O is sufficiently nucleophilic to break the P–O bonds.^{27,28} The evidence for the bridging hydrogen in **6a** came from the ^1H NMR spectrum of the reaction that showed a singlet at 14.9 ppm.²⁹ In addition, a broad resonance at -1.66 ppm suggested that the chloride on the nickel center was displaced by OH^- to yield a nickel hydroxide complex.³⁰ Both **5a** and **6a** proved to be unstable in the basic medium; extended reaction time led to the decomposition of

(27) Salem, H.; Shimon, L. J. W.; Diskin-Posner, Y.; Leitus, G.; Ben-David, Y.; Milstein, D. *Organometallics* **2009**, *28*, 4791–4806.

(28) None of the nickel complexes reported here react with H_2O at 80°C in $\text{DMF-}d_7$.

(29) (a) Werner, H.; Feser, R. Z. *Anorg. Allg. Chem.* **1979**, *458*, 301–308. (b) Werner, H.; Khac, T. N. Z. *Anorg. Allg. Chem.* **1981**, *475*, 241–250. (c) Christiansen, A.; Selent, D.; Spannenberg, A.; Baumann, W.; Franke, R.; Börner, A. *Organometallics* **2010**, *29*, 3139–3145.

(30) (a) Cámpora, J.; Palma, P.; del Río, D.; Álvarez, E. *Organometallics* **2004**, *23*, 1652–1655. (b) Cámpora, J.; Palma, P.; del Río, D.; Conejo, M. M.; Álvarez, E. *Organometallics* **2004**, *23*, 5653–5655.

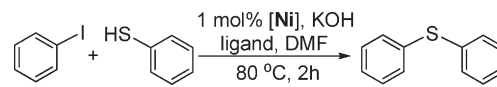
Scheme 3. Reaction of 1a with KOH in DMF-*d*₇ at 80 °C**Scheme 4. Reaction of 3a (or 4a) with KOH in DMF-*d*₇ at 80 °C**

these complexes to a very complicated mixture of phosphorus-containing products (in the range from -10 to 50 ppm). A separate NMR experiment mixing KOH and $\text{Ph}_2\text{P}(\text{O})\text{H}$ in $\text{DMF-}d_7$ at 80 °C confirmed that one of the degradation products was Ph_2POK , and it was further decomposed to PPh_3 as well as other unidentified products. The formation of PPh_3 was perplexing to us; however, it was genuinely produced during the reaction. The concentration of PPh_3 increased over time, and its identity was repeatedly confirmed by $^{31}\text{P}\{^1\text{H}\}$ NMR (-5.8 ppm) and GC/MS (fw: 262).

We also examined whether or not the P–O bonds in nickel thiolate complexes were susceptible to the attack of KOH under similar reaction conditions. The reaction of **3a** with KOH exhibited two AB spin systems in the $^{31}\text{P}\{^1\text{H}\}$ NMR spectrum. While one of them was identical to the one shown for **6a**, the other one ($\nu_A = 147.5$ ppm, $\nu_B = 132.3$ ppm, $J_{AB} = 403$ Hz) was tentatively attributed to the resonances for a new thiolate complex with an analogous seven-membered ring established by the hydrogen bonding (Scheme 4). Similarly, the reaction of **4a** with KOH generated **6a** and a new species ($\nu_A = 148.2$ ppm, $\nu_B = 133.2$ ppm, $J_{AB} = 401$ Hz) presumably with the thiolate ligand still attached to the nickel center. In any case, the nickel pincer complex was ultimately degraded to a very complicated mixture containing both Ph_2POK and PPh_3 . Because this process was accelerated by added KOH, we believed that our catalytic conditions with a much larger KOH to Ni ratio (200:1) would favor a more rapid decomposition of the pincer complexes. We also attempted to investigate the fate of the pincer backbone by GC/MS. Unfortunately, the spectra were too complicated to provide conclusive information.³¹

Mechanistic Considerations. In view of the recent report that residual copper in FeCl_3 catalyzes various coupling reactions,¹² we replaced **1a** (for the reaction in entry 1, Table 3) with 10 mol % of anhydrous NiCl_2 , which was used as the precursor for the synthesis of **1a–d**. No significant cross-coupling product was observed, confirming that the reactions in Table 3 were indeed catalyzed by **1a**.

(31) Peaks in the GC diagram with m/z ratios of 110, 154, 186, 278, and 294 were seen in each case. They are consistent with formulas of $\text{C}_6\text{H}_4(\text{OH})_2$, $(\text{C}_6\text{H}_5)_2$, $(\text{C}_6\text{H}_4\text{OH})_2$, $\text{C}_6\text{H}_5\text{OPPh}_2$, and $\text{C}_6\text{H}_4(\text{OH})(\text{OPPh}_2)$.

Table 4. Thiolation of Iodobenzene Catalyzed by Various Combinations of Nickel Sources and Ligands^a

entry	[Ni]	ligand	GC yield (%)
1	NiCl_2	PPh_3 (10 mol %)	33
2	NiCl_2	$\text{Ph}_2\text{P}(\text{O})\text{H}$ (10 mol %)	85
3	$\text{Ni}(\text{COD})_2$	PPh_3 (10 mol %)	41
4	$\text{Ni}(\text{COD})_2$	$\text{Ph}_2\text{P}(\text{O})\text{H}$ (10 mol %)	93
5	$\text{Ni}(\text{COD})_2$	$\text{Ph}_2\text{P}(\text{O})\text{H}$ (2 mol %)	97

^a Reaction conditions: 1.0 mmol of PhSH , 1.1 mmol of PhI , 2.0 mmol of KOH, and 1.0 mmol of *n*-decane (GC internal standard) in 6 mL of solvent.

Now that we have ruled out the possibility of nickel thiolate complexes being directly involved in the C–S bond-forming step, there are a few other unaddressed mechanistic issues: Is the active catalyst Ni(II) or Ni(0), and does Ph_2POK or PPh_3 play any role in promoting the catalytic reactions? To answer these questions, we used NiCl_2 and $\text{Ni}(\text{COD})_2$ ($\text{COD} = 1,5$ -cyclooctadiene) as the nickel sources and mixed them with $\text{Ph}_2\text{P}(\text{O})\text{H}$ and PPh_3 as precatalysts for C–S coupling reactions (entries 1–4, Table 4). The best combination was proven to be a Ni(0) species with $\text{Ph}_2\text{P}(\text{O})\text{H}$ as the supporting ligand. When the Ni to ligand ratio was maintained at 1:2, the GC yield of the sulfide product (entry 5, Table 4) was comparable to that seen in **1a**-catalyzed cross-coupling reactions.

There are lengthy discussions in the literature about nanoparticles released from catalyst degradation being the true catalysts, particularly in Pd-catalyzed Heck, Suzuki, and related coupling reactions.³² Under these conditions where Pd(0) is not sufficiently protected by ligand, the addition of metallic mercury leads to the amalgamation of nanoparticles, thereby decelerating or even shutting down the reactions.³³ The same approach has been successfully utilized to deactivate nickel nanoparticles in catalytic transfer hydrogenation of ketones.³⁴ To explore this mechanistic possibility, we used GC/MS to monitor the progress of Ni-catalyzed coupling of PhI and PhSH with and without added mercury and examined the GC yield of the coupling product as a function of time (Figure 8). As a comparison, the catalytic activity of $\text{Ni}(\text{COD})_2/\text{Ph}_2\text{P}(\text{O})\text{H}$ was also illustrated in Figure 8. The fact that mercury had no effect on the catalytic performance of **1a** suggested that the coupling reaction was catalyzed by a homogeneous metal–complex solution. The catalysis with **1a** clearly showed an induction period, and the C–S coupling reaction was complete after 60 min.

(32) (a) Widegren, J. A.; Finke, R. G. *J. Mol. Catal. A: Chem.* **2003**, *198*, 317–341. (b) Phan, N. T. S.; Van Der Sluys, M.; Jones, C. W. *Adv. Synth. Catal.* **2006**, *348*, 609–679. (c) Astruc, D. *Inorg. Chem.* **2007**, *46*, 1884–1894. (d) Tsuji, Y.; Fujihara, T. *Inorg. Chem.* **2007**, *46*, 1895–1902.

(33) (a) Consorti, C. S.; Zanini, M. L.; Leal, S.; Ebeling, G.; Dupont, J. *Org. Lett.* **2003**, *5*, 983–986. (b) Eberhard, M. R. *Org. Lett.* **2004**, *6*, 2125–2128. (c) Yu, K.; Sommer, W.; Richardson, J. M.; Weck, M.; Jones, C. W. *Adv. Synth. Catal.* **2005**, *347*, 161–171. (d) Bergbreiter, D. E.; Osburn, P. L.; Frels, J. D. *Adv. Synth. Catal.* **2005**, *347*, 172–184. (e) Sommer, W. J.; Yu, K.; Sears, J. S.; Ji, Y.; Zheng, X.; Davis, R. J.; Sherrill, C. D.; Jones, C. W.; Weck, M. *Organometallics* **2005**, *24*, 4351–4361. (f) Olsson, D.; Nilsson, P.; El Masnaouy, M.; Wendt, O. F. *Dalton Trans.* **2005**, 1924–1929. (g) Lipke, M. C.; Woloszynek, R. A.; Ma, L.; Protasiewicz, J. D. *Organometallics* **2009**, *28*, 188–196.

(34) Alonso, F.; Riente, P.; Sirvent, J. A.; Yus, M. *Appl. Catal., A* **2010**, *378*, 42–51.

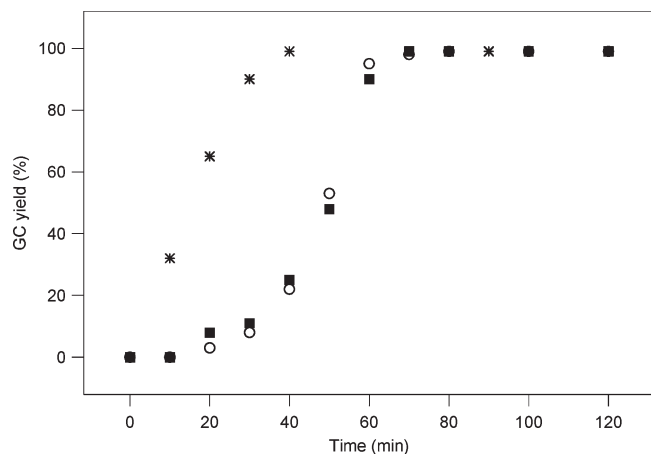


Figure 8. GC yield of Ph₂S as a function of time [reaction conditions: 0.17 M of PhSH, 0.18 M of PhI, 0.34 M of KOH, and nickel catalyst in DMF at 80 °C; ■, 1 mol % of **1a**; ○, 1 mol % of **1a** with 125 mol % of metallic Hg; *, 1 mol % of Ni(COD)₂ with 2 mol % of Ph₂P(O)H].

In contrast, the reaction catalyzed by Ni(COD)₂/Ph₂P(O)H finished within 40 min with no observable induction period. Although the mechanistic details of our nickel pincer system are still not fully understood due to the complex decomposition process for the catalysts (or more precisely, the pre-catalysts), we favor a mechanism involving a Ni(0) species supported by Ph₂PO⁻.³⁵ The proposed active catalyst could be generated from the attack of KOH on the pincer complexes, as seen in Schemes 3 and 4. The difference in the catalytic activity of **1a–d** probably reflects how easily the P–O bonds are cleaved by KOH; the more bulky ^tBu groups in **1d** induce a slower decomposition process and presumably generate a smaller amount of active catalyst during the same period of time. The Ni(0)-catalyzed C–S coupling reactions potentially follow a three-step mechanism comprised of (1) the oxidative addition of an aryl iodide to a Ni(0) center, (2) the substitution reaction between the resulting nickel iodide complex and ArS⁻, and (3) the reductive elimination of the sulfide product from the Ni(II) center. A similar reaction pathway has been extensively studied in Pd-catalyzed C–S coupling reactions.³⁶ Comparative studies in Table 4 (entries 4, 5) also suggested that excess Ph₂P(O)H could be detrimental to the chemical yield, possibly due to the metal center being saturated by the ligand to disfavor the oxidative addition step.

Secondary phosphine oxides are known to promote Pd-catalyzed cross-coupling reactions.^{8d,e,37} Related nickel systems such as Ni(COD)₂/^tBu₂P(O)H work particularly well for catalytic Kumada–Corriu reactions,^{8d,38} but, prior to our work, had not been employed in catalyzing other cross-coupling reactions. Although secondary phosphine oxides are attractive ligands for catalysis due to the air stability,

their decomposition in the presence of a base at a modest temperature could be a concern, as demonstrated in the case of Ph₂P(O)H (see Schemes 3 and 4). In fact, we were curious about whether our nickel catalysts were still alive after the catalytic reactions. After the reactions in Figure 8 were complete, we added more substrates to reach their initial concentrations, replenished the consumed KOH (1 equiv), and reexamined the catalytic efficiency. The GC yields in the second run dropped significantly (from 99% to 10% for **1a** and from 99% to 47% for Ni(COD)₂/Ph₂P(O)H), confirming that the active catalysts were partially, if not totally, converted to catalytically inactive species.

Conclusions

Inspired by the work of Morales-Morales et al.,^{5a} we have developed an efficient nickel pincer system for the catalytic cross-coupling of aryl iodides and thiols in the presence of KOH. The improved method has been used to produce a variety of diaryl sulfides in high yield and free of homo-coupling products. NMR studies have shown the formation of nickel thiolate complexes during the catalytic process; however, they react with KOH to generate active catalysts rather than participate directly in the C–S bond-forming step. Further mechanistic investigations have ruled out the possibility of nickel nanoparticles or copper contaminants acting as the real catalysts. The cross-coupling reactions are more likely to be catalyzed by secondary phosphine oxide-ligated Ni(0) species, which can be available from catalyst degradation. Further studies have suggested that the nickel pincer complexes are converted to less reactive catalytic mixtures, preventing the catalysts from being reused.

Experimental Section

General Comments. All the organometallic compounds were prepared and handled under an argon atmosphere using standard Schlenk and inert-atmosphere box techniques. Complexes **1a–d**, **2a**, **3a**, and **4a** may be exposed to air without much decomposition. Dry and oxygen-free solvents (THF, toluene, and pentane) were collected from an Innovative Technology solvent purification system and used throughout the experiments. DMF was degassed by bubbling argon through the solvent for 15 min prior to use. Benzene-*d*₆ was distilled from Na and benzophenone under an argon atmosphere. All other solvents (CH₂Cl₂, *n*-hexane, hexanes, CD₂Cl₂, and CDCl₃) were obtained from commercial sources and used without purification. [2,6-(Ph₂PO)₂C₆H₃]NiCl (**1a**),^{5a} [2,6-(ⁱPr₂PO)₂C₆H₃]NiCl (**1c**),^{4d} and [2,6-(^tBu₂PO)₂C₆H₃]NiCl (**1d**)^{5d} were prepared as described in the literature.

[2,6-(Me₂PO)₂C₆H₃]NiCl (**1b**). To a stirring solution of resorcinol (110 mg, 1.0 mmol) in 10 mL of THF was slowly added NaH (48 mg, 2.0 mmol) at room temperature over a period of 10 min. The resulting mixture was refluxed for 1 h, followed by the addition of Me₂PCL (193 mg, 2.0 mmol). After refluxing for another hour, a suspension of anhydrous NiCl₂ (130 mg, 1.0 mmol) in 40 mL of toluene was added via cannula, and the reaction mixture was further refluxed for 30 h. Solvent was removed under vacuum, and the residue was extracted with CH₂Cl₂. Removal of CH₂Cl₂ under vacuum afforded **1b** as a yellow air-stable solid (200 mg, 62% yield). Single crystals of **1b** were grown by adding *n*-hexane to a saturated CH₂Cl₂ solution of the complex. ¹H NMR (400 MHz, CDCl₃, δ): 7.02 (t, *Ar*, J_{H–H} = 8.0 Hz, 1H), 6.43 (d, *Ar*, J_{H–H} = 8.0 Hz, 2H), 1.88 (virtual triplet, CH₃, J_{P–H} = 5.4 Hz, 12H). ¹³C{¹H} NMR (101 MHz, CDCl₃, δ): 167.1 (t, J_{C–P} = 12.2 Hz), 129.5, 126.6 (t, J_{C–P} = 23.1 Hz), 106.1 (t, J_{C–P} = 7.0 Hz), 16.7 (t, J_{C–P} = 13.1 Hz, CH₃). ³¹P{¹H}

(35) Ph₂P(O)H was reported to add oxidatively to Pt(PPh₃)₄ to generate a Pt(II) hydride complex. For details, see: Beaulieu, W. B.; Rauchfuss, T. B.; Roundhill, D. M. *Inorg. Chem.* **1975**, *14*, 1732–1734. We believed that, in the presence of KOH, Ph₂P(O)H would be deprotonated and the nickel center would have a formal oxidation state of zero.

(36) Alvaro, E.; Hartwig, J. F. *J. Am. Chem. Soc.* **2009**, *131*, 7858–7868.

(37) For reviews, see: (a) Ackermann, L. *Synthesis* **2006**, 1557–1571. (b) Ackermann, L.; Born, R.; Spatz, J. H.; Althammer, A.; Gschrei, C. J. *Pure Appl. Chem.* **2006**, *78*, 209–214.

(38) Wolf, C.; Xu, H. *J. Org. Chem.* **2008**, *73*, 162–167.

NMR (162 MHz, CDCl_3 , δ): 160.6. Anal. Calcd for $\text{C}_{10}\text{H}_{15}\text{P}_2\text{O}_2\text{NiCl}$: C, 37.15; H, 4.68; Cl, 10.97. Found: C, 37.12; H, 4.65; Cl, 10.89.

General Procedures for Catalytic Cross-Coupling of Aryl Iodides and Thiols. To a 10 mL scintillation vial under an argon atmosphere was added 1.0 mmol of thiol, 1.1 mmol of aryl iodide, 2.0 mmol of KOH, 0.01 mmol of nickel catalyst, and 6 mL of DMF. When GC yield was desired, 1.0 mmol of *n*-decane was also added as an internal standard. The vial was sealed and then heated at 80 or 130 °C until there was no thiol left (monitored by withdrawing aliquots and analyzed by GC-MS). The solvent was removed under vacuum, and the residue was extracted with CH_2Cl_2 . The combined CH_2Cl_2 layers were passed through a short pad of silica gel and concentrated under vacuum to afford the crude product. The sulfide product was further purified by flash column chromatography. All the isolated diaryl sulfide products were characterized by ^1H NMR and $^{13}\text{C}\{^1\text{H}\}$ NMR spectroscopy (see the Supporting Information), and their NMR data were consistent with the literature values.

[2,6-(Ph₂PO)₂C₆H₃]NiSPh (2a). At -78 °C under an argon atmosphere, **1a** (200 mg, 0.35 mmol) and NaSPh (90%, technical grade, purchased from Sigma-Aldrich, 51 mg, 0.35 mmol) were mixed in 20 mL of THF. The resulting mixture was warmed to room temperature and stirred overnight. The solvent was then removed under vacuum, and the reddish residue was triturated with pentane. The material remaining after trituration was treated with 20 mL of toluene, filtered through a pad of Celite, and concentrated under vacuum. The product was further purified via recrystallization from toluene/pentane and isolated as a red crystalline solid (180 mg, 80% yield). X-ray quality crystals were grown by allowing a layer of pentane to slowly diffuse into a saturated toluene solution of **2a**. ^1H NMR (400 MHz, CD_2Cl_2 , δ): 7.83–7.78 (m, *Ar*, 8H), 7.53–7.49 (m, *Ar*, 4H), 7.43–7.40 (m, *Ar*, 8H), 7.08 (t, *Ar*, $J_{\text{H-H}} = 8.0$ Hz, 1H), 6.99 (d, *Ar*, $J_{\text{H-H}} = 8.0$ Hz, 2H), 6.65–6.61 (m, *Ar*, 3H), 6.49 (t, *Ar*, $J_{\text{H-H}} = 8.0$ Hz, 2H). $^{13}\text{C}\{^1\text{H}\}$ NMR (101 MHz, CDCl_3 , δ): 166.3 (t, $J_{\text{C-P}} = 11.1$ Hz), 143.7 (t, $J_{\text{C-P}} = 7.0$ Hz), 134.0, 132.8, 132.6, 132.3 (t, $J_{\text{C-P}} = 7.0$ Hz), 131.5, 129.6, 128.6 (t, $J_{\text{C-P}} = 6.0$ Hz), 127.2, 122.9, 106.2 (t, $J_{\text{C-P}} = 7.0$ Hz). $^{31}\text{P}\{^1\text{H}\}$ NMR (162 MHz, CD_2Cl_2 , δ): 149.0. Anal. Calcd for $\text{C}_{36}\text{H}_{28}\text{P}_2\text{O}_2\text{NiS}$: C, 67.00; H, 4.37. Found: C, 67.04; H, 4.29.

[2,6-(Ph₂PO)₂C₆H₃]NiSC₆H₄CH₃ (3a). To a mixture of sodium hydride (48 mg, 2.0 mmol) and THF (30 mL) was added 4-methylbenzenethiol (248 mg, 2.0 mmol) at 0 °C under an argon atmosphere. The resulting mixture was warmed to room temperature and stirred for 1 h before **1a** (572 mg, 1.0 mmol) was added. After stirring at room temperature for another 2 h, the volatiles were removed under vacuum and the residue was extracted with toluene and filtered through a pad of Celite. Removal of toluene under vacuum resulted in a red solid, which was recrystallized from CH_2Cl_2 /hexanes (1:2) to produce red crystals of **3a** (508 mg, 77% yield). ^1H NMR (400 MHz, CDCl_3 , δ): 7.84–7.80 (m, *Ar*, 8H), 7.48–7.35 (m, *Ar*, 12H), 7.07 (t, $J_{\text{H-H}} = 7.9$ Hz, *Ar*, 1H), 6.91 (d, $J_{\text{H-H}} = 7.9$ Hz, *Ar*, 2H), 6.64 (d, $J_{\text{H-H}} = 7.9$ Hz, *Ar*, 2H), 6.24 (d, $J_{\text{H-H}} = 7.9$ Hz, *Ar*, 2H), 2.01 (s, CH_3 , 3H). $^{13}\text{C}\{^1\text{H}\}$ NMR (101 MHz, CDCl_3 , δ): 166.2 (t, $J_{\text{C-P}} = 11.1$ Hz), 139.7 (t, $J_{\text{C-P}} = 8.0$ Hz), 133.9, 132.8, 132.6, 132.5, 132.3 (t, $J_{\text{C-P}} = 7.2$ Hz), 131.3, 129.4, 128.5 (t, $J_{\text{C-P}} = 5.3$ Hz), 128.0, 106.1 (t, $J_{\text{C-P}} = 6.7$ Hz), 20.8 (CH_3). $^{31}\text{P}\{^1\text{H}\}$ NMR (162 MHz, CDCl_3 , δ): 148.5. Anal. Calcd for $\text{C}_{37}\text{H}_{30}\text{NiO}_2\text{P}_2\text{S}$: C, 67.40; H, 4.59. Found: C, 67.34; H, 4.49.

[2,6-(Ph₂PO)₂C₆H₃]NiSC₆H₄OCH₃ (4a) was prepared in 64% yield by a procedure similar to that used for **3a**. X-ray-quality crystals of **4a** were obtained from the recrystallization of **4a** in CH_2Cl_2 /hexanes. ^1H NMR (400 MHz, CDCl_3 , δ): 7.86–7.82 (m, *Ar*, 8H), 7.50–7.38 (m, *Ar*, 12H), 7.07 (t, $J_{\text{H-H}} = 7.9$ Hz,

Ar, 1H), 6.92 (d, $J_{\text{H-H}} = 8.7$ Hz, *Ar*, 2H), 6.65 (d, $J_{\text{H-H}} = 7.9$ Hz, *Ar*, 2H), 6.05 (d, $J_{\text{H-H}} = 8.7$ Hz, *Ar*, 2H), 3.58 (s, OCH_3 , 3H). $^{13}\text{C}\{^1\text{H}\}$ NMR (101 MHz, CDCl_3 , δ): 166.2 (t, $J_{\text{C-P}} = 11.1$ Hz), 156.3, 134.9, 133.8 (t, $J_{\text{C-P}} = 8.6$ Hz), 132.8, 132.6, 132.3 (t, $J_{\text{C-P}} = 7.0$ Hz), 131.4, 129.4, 128.5 (t, $J_{\text{C-P}} = 5.2$ Hz), 113.0, 106.2 (t, $J_{\text{C-P}} = 6.6$ Hz), 55.0 (OCH_3). $^{31}\text{P}\{^1\text{H}\}$ NMR (162 MHz, CDCl_3 , δ): 149.1. Anal. Calcd for $\text{C}_{37}\text{H}_{30}\text{NiO}_3\text{P}_2\text{S}$: C, 65.80; H, 4.48. Found: C, 65.40; H, 4.43.

Independent Synthesis of [2,6-(Ph₂PO)₂C₆H₃]NiP(O)Ph₂ (5a). $\text{Ph}_2\text{P(O)H}$ (202 mg, 1.0 mmol) was dissolved in 30 mL of THF under an argon atmosphere, and KOH (56 mg, 1.0 mmol) was added. The mixture was stirred at room temperature for 16 h, after which the solvent was removed under vacuum. The resulting white solid was mixed with **1a** (200 mg, 0.35 mmol) in 30 mL of toluene and refluxed under argon for 6 h. The mixture was then cooled to room temperature and filtered through a pad of Celite. Removal of toluene under vacuum afforded a yellow solid, which was washed with pentane (20 mL \times 3) to produce **5a**, showing >95% pure by NMR (110 mg, 43% yield). X-ray quality crystals of **5a** were obtained from evaporating the benzene-*d*₆ solution of **5a**. ^1H NMR (400 MHz, C_6D_6 , δ): 8.05–7.95 (m, *Ar*, 8H), 7.57–7.53 (m, *Ar*, 4H), 7.10–7.04 (m, *Ar*, 13H), 6.91–6.79 (m, *Ar*, 8H). $^{13}\text{C}\{^1\text{H}\}$ NMR (101 MHz, C_6D_6 , δ): 166.2 (t, $J_{\text{C-P}} = 9.3$ Hz, *Ar*), 145.7 (d, $J_{\text{C-P}} = 39.1$ Hz), 132.9 (t, $J_{\text{C-P}} = 6.9$ Hz), 132.3 (t, $J_{\text{C-P}} = 26.5$ Hz), 131.3, 131.2, 130.4 (d, $J_{\text{C-P}} = 11.3$ Hz), 128.4 (t, $J_{\text{C-P}} = 5.3$ Hz), 127.9, 127.7, 127.3 (d, $J_{\text{C-P}} = 9.4$ Hz), 106.4 (t, $J_{\text{C-P}} = 5.9$ Hz). $^{31}\text{P}\{^1\text{H}\}$ NMR (162 MHz, C_6D_6 , δ): 152.7 (d, $^2J_{\text{P-P}} = 53.7$ Hz, pincer OPPh_2 , 2P), 64.9 (t, $^2J_{\text{P-P}} = 53.7$ Hz, NiP(O)Ph_2 , 1P). IR (in toluene): 1178 cm^{-1} (P=O). This complex decomposed rapidly upon standing, precluding reliable elemental and mass spectral analyses.

X-ray Structure Determinations. Crystal data collection and refinement parameters are summarized in Table 1. Intensity data were collected at 150 K on a Bruker SMART6000 CCD diffractometer using graphite-monochromated Cu $K\alpha$ radiation, $\lambda = 1.54178$ Å. The data frames were processed using the program SAINT. The data were corrected for decay, Lorentz and polarization effects, as well as absorption and beam corrections based on the multiscan technique used in SADABS. The structures were solved by a combination of direct methods in SHELXTL and the difference Fourier technique and refined by full-matrix least-squares procedures. Non-hydrogen atoms were refined with anisotropic displacement parameters. The H-atoms were either located or calculated and subsequently treated with a riding model. Compound **1b** crystallized as two independent molecules in the lattice with minimal variation in conformation. Complex **4a** crystallized as both plates and needles showing different unit cell parameters. Compound **5a** cocrystallized with the solvent molecule (C_6D_6).

Acknowledgment. We thank the National Science Foundation (CAREER Award CHE-0952083 and NSF-REU program CHE-0754114) and the donors of the American Chemical Society Petroleum Research Fund (49646-DNI3) for support of this research. J.Z. thanks the University of Cincinnati University Research Council for a postdoctoral research fellowship. X-ray data were collected on a Bruker SMART6000 diffractometer that was purchased with funding provided by an NSF-MRI grant (CHE-0215950).

Supporting Information Available: NMR spectra of the isolated sulfide compounds and X-ray crystallographic data in CIF format. This material is available free of charge via the Internet at <http://pubs.acs.org>.